Environmental Science & Technology

pubs.acs.org/est

Article

Nanoactivated Carbon Reduces Mercury Mobility and Uptake by *Oryza sativa L*: Mechanistic Investigation Using Spectroscopic and Microscopic Techniques

Jianxu Wang,* Sabry M. Shaheen, Christopher W. N. Anderson, Ying Xing, Shirong Liu, Jicheng Xia, Xinbin Feng,* and Jörg Rinklebe

Cite This: *Environ. Sci. Technol.* 2020, 54, 2698−2706

Read Online

ACCESS | Metrics & More | Article Recommendations | Supporting Information

ABSTRACT: Mercury (Hg) contamination of paddy field poses a health risk to rice consumers, and its remediation is a subject of global scientific attention. In recent years focus has been given to in situ techniques which reduce the risk of Hg entering the food chain. Here, we investigate the use of nanoactivated carbon (NAC) as a soil amendment to minimize Hg uptake by rice plants. Application of 1−3% NAC to soil (by weight) reduced Hg concentration in the pore water (by 61−76%) and its bioaccumulation in the tissues of rice plants (by 15−63%), relative to the corresponding control. Specifically, NAC reduced the Hg concentration of polished rice by 47−63% compared to the control, to a level that was 29−49% lower than the food safety value (20 ng g^{-1}) defined by the Chinese government. The NAC induced a change in Hg binding from organic matter to nano-HgS in the soil as a function of soil amendment. This Hg speciation transformation might be coupled to the reduction of sulfoxide to reduced sulfur species (S^0) by NAC. The NAC amendment may be a practical and effective solution to mitigate the risk of Hg transferring from contaminated soil to rice grains at locations around the world.

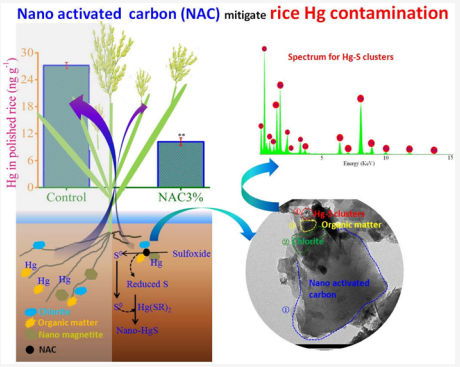

INTRODUCTION

Mercury (Hg) is a persistent toxic element in soil and sediment, which can bioaccumulate in both terrestrial and aquatic food webs.[1,2] Together with its methylated form MeHg, Hg is ranked as a top six global pollutant with remediation a key priority to mitigate ecological risk at contaminated sites worldwide.[3−5]

The bioaccumulation of Hg in paddy field ecosystems has become a critical environmental problem worldwide[6] and is particularly apparent in Asia where 1200 tons of Hg is estimated to be released to the environment annually. Asia is also a continent where over 600 million tons of rice is produced annually[7] and rice paddy fields can become contaminated with Hg through irrigation with contaminated river water, deposition of atmospheric Hg, and the application of Hg-containing fertilizers and pesticides.[8]

Due to a lack of appropriate techniques and regulations, as well as a lack of funding for environmental cleanup, poor management of Hg-contaminated paddy fields can result in rice crop Hg concentrations higher than the maximum permissible level of Hg in food defined by governmental organizations. Mercury remediation is expensive. Methods such as capping with inert or active materials, excavation, soil washing, and thermal desorption[9,10] have been developed to reduce the exposure risk of Hg in soils and sediments. However, such methods have limited application to productive agricultural soil due to high cost, and the degradation of soil physical, chemical, and biological properties that can result from remediation.[11] Recent studies have shown that immobilization is a better approach to manage the risk of bioavailable Hg in paddy soil.[12−14] Selenium compounds,[12,15] elemental sulfur, and sulfate[16] have been shown to immobilize Hg when used as a soil amendment although their application beyond laboratory scale is limited. The lack of any proven, reliable, and high-efficiency immobilization technology remains a key barrier for the use of such technology to manage the risk of Hg in productive farmlands.

Activated carbon is an environmentally friendly alternative soil amendment for Hg immobilization that is already widely used in agronomy and industry.[17] Activated carbon can be used as a sorbent to immobilize or remove toxic elements and organic pollutants from water, industrial effluents, and soils.[18,19] Also, activated carbon has previously been shown to have good potential to reduce total dissolved Hg and MeHg bioavailability in Hg-contaminated sediments.[20] Possible mechanisms are Hg sorption to functional groups on the

Received: September 20, 2019
Revised: January 3, 2020
Accepted: February 11, 2020
Published: February 11, 2020

carbon's surface (e.g., thiols), and the formation of stable Hg complexes.[21] Activated carbon has a high sorption capacity for dissolved organic matter (DOM), and this might explain immobilization of Hg bound to soil DOM.[22] Alternatively, Hg(I) can precipitate on the surface of activated carbon.[23] The addition of activated carbon to soil may enhance the formation of soil aggregates.[24,25] The effect of activated carbon on soil structure may have an impact on trace element bioavailability. Nanoscaled activated carbon may be even more efficient in Hg sorption because of their high surface area-to-volume ratio, chemical reactivity, and unique functionalities.[17] However, despite the promise, the mechanism and large-scale feasibility of using nanoactivated carbon (NAC) to remediate Hg-contaminated soil has yet to be studied.

In the current work we have used nanoactivated carbon (NAC; average diameter 40 nm) as an amendment to treat Hg-contaminated paddy soil. We hypothesize that NAC may decrease Hg bioavailability in the soil through adsorption and precipitation, and enhanced formation of soil microaggregates, as well as Hg accumulation by rice plants. To verify our hypothesis, we aimed to (1) quantify the effect of NAC amendment on rice plant growth, and pore water chemistry (total dissolved Hg, dissolved organic carbon, pH, redox potential and sulfate); (2) investigate the ability of NAC to reduce pore water Hg concentrations and mitigate the bioaccumulation of Hg by rice plants (root, stalk, leaf, and grains); and (3) propose potential mechanisms of Hg immobilization by NAC amendment using integrated spectroscopic and microscopic techniques. Specifically, we investigated changes of soil microaggregates constituents using transmission electron microscopy coupled with energy dispersive X-ray (TEM-EDX) spectroscopy. Also, we characterized Hg and sulfur speciation in the soils using synchrotron-based Hg L_3-edge XANES and S K-edge XANES spectroscopy. We used a combination of biogeochemical and spectroscopic approaches to elucidate and determine the fundamental mechanisms which control the speciation and immobilization of Hg in nanoactivated carbon treated paddy soil.

MATERIALS AND METHODS

Sampling, Preparation, and Characterization of the Studied Soil and Nanoactivated Carbon. A composite bulk soil sample (500 kg) was collected from 0 to 20 cm depth at random locations across 100 m^2 of contaminated farmland at Wanshan Hg mine (WSHM) in China. The farmland was previously used for rice cultivation and had been ploughed immediately prior to sampling. The soils were transported to the laboratory where they were air-dried, crushed, and passed through a 2 mm nylon sieve prior to use. The analytical methods for soil pH, total Hg, carbon, nitrogen, sulfur, and iron (Fe) contents, as well as Fe speciation are given in the Supporting Information (SI, S1.1).[28,29] The studied soil is neutral (pH = 7.5 ± 0.2), with total carbon, nitrogen, sulfur, and iron contents of 20, 2.1, 1.0, and 22 g kg^{-1}, respectively (SI Table S1). Iron speciation characterized by Fe L-edge X-ray near edge structure (XANES) spectroscopy shows this element to be mainly present as α-Fe_2O_3 (Figure S1). The average total Hg concentration in the soil is 129 mg kg^{-1}, which is 86 times greater than the maximum allowable Hg concentration (1.5 mg kg^{-1}) for farmland defined by the Chinese government,[26] and is greater than the trigger point (1.5−10 mg kg^{-1}) suggested by Kabata-Pendias[27] for remedial action.

The studied nanoactivated carbon (product No. MH-C-40) was purchased from Nanjing Emperor Nano Materials Co., LTD in China. The analytical methods for total carbon, and specific surface area of the nanoactivated carbon (NAC), as well as electron microphotograph are given in the SI (S1.2). Total carbon content of the NAC is 99.5%, and its specific surface area is 500 m^2 g^{-1} (Table S2). An electron microphotograph of the NAC is shown in the SI (Figure S2). According to the producer, the diameter of particle size of the NAC ranged between 20 and 50 nm with an average of 40 nm, and its density is 3.02 g m^{-3}.

Pot Experiment. Plastic pots (volume, 5L) were purchased for rice incubation and cleaned with 5% HNO_3 and purified water prior to use. Pots were divided into three groups, with three replicates in each group. Pots in the first group were filled with 3600 g of field soil (Control); pots in the second group were filled with 3564 g of field soil and 36 g of nanoactivated carbon (1% NAC); pots in the third group were filled with 3492 g of field soil and 108 g of nanoactivated Carbon (3% NAC). To mix NAC and soil, preparations were transferred into a 10-L plastic bag, and manually shaken for 20 min before pot filling. The soil became weakly dark and no visual NAC aggregates were observed after shaking. All pots were randomly arranged, irrigated with purified water (total Hg < 0.02 ng L^{-1}) at the Guizhou Rice Research Institute, and flooding was maintained at 3 cm in depth during an equilibration period of 5 days.

Rice seedlings (30-day old) with similar biomass and length were selected from a rice seedling incubation paddy field at the Guizhou Rice Research Institute (GRRI). Two seedlings were transplanted into each pot, and these were maintained for 120 days. To support plant growth, urea (CON_2H_4) was supplied to each pot at a dose of 56 mg kg^{-1}, 70 mg kg^{-1}, and 56 mg kg^{-1} prior to transplanting, at the tillering stage, and at the panicle stage, respectively, as recommended by the researchers from GRRI. Purified water was regularly supplied to each pot to maintain the depth of overlying water at 3 cm throughout the rice growing season.

Sample Collection, Preparation, And Analysis. About 100 mL of pore water in each pot was collected on days 5, 30, 50, 70, 80, 100, and 118 after transplanting using a passive pore water sampler (pore size Φ = 10-μm; Daxiong Monitor Co., Shenzhen, China). Each bulk sample was divided into three subsamples for total dissolved Hg, sulfate, and dissolved organic carbon (DOC) analysis. Rice plants and their paired soil samples were collected on Day 120, and stored in 10L nylon bags and 500 mL Ziplock bags, respectively. Whole rice plants were pulled from the pots; soil attached to the roots was collected by hand (with rubber gloves) and sealed in 1L Ziplock bags. In the laboratory, rice plants were cleaned with running tap water, and thereafter with deionized water. Each rice plant was separated into root, stalk, leaf, and panicle sections using stainless-steel scissors. Root sections were further cleaned with 0.01 M ethylenediaminetetraacetic acid (EDTA) and deionized water.

All plant tissues were freeze-dried by a lyophilizer (Fd-1−50, Boyikang Co., Beijing, China) at −50 °C and 12 Pa for 96 h. The dried panicle was divided into the hull, bran, and polished rice. Plant tissues were crushed to powder using an electrical microcrusher (IKA-Werke GmbH & Co., Staufen, Germany). Soil samples were kept at −18 °C prior to freeze-drying using a lyophilizer (Fd-1−50, Boyikang Co., Beijing, China) at −50 °C and 12 Pa for 192 h. Each sample was subsequently

https://dx.doi.org/10.1021/acs.est.9b05685
Environ. Sci. Technol. 2020, 54, 2698−2706

homogenized using an agate mortar. The microcrusher and agate mortar were carefully cleaned after processing each sample to avoid any cross-contamination. Processed soil and plant samples were stored in a refrigerator at +4 °C prior to being analyzed for Hg concentrations. The methods for total dissolved Hg, sulfate, DOC, oxidation−reduction potential (ORP), and pH analysis for pore water samples are described in the SI (section S1.3). The methods for plant total Hg analysis are shown in the SI (section S1.4).[30] The methods for recording plant biomass are described in the SI (section S1.4).

Mercury L_3-Edge and Sulfur K-Edge X-ray Absorption Near Edge Structure (XANES) Spectroscopy. *Mercury L_3-Edge XANES Spectroscopy.* About 0.1 g freeze-dried soil powder from the control and 3% NAC treatment was pressed into a thin pellet (Φ = 1 cm) using a manual hydraulic press (FW-4, Tianguang instrument, China) for analysis. The Hg reference compounds cinnabar (α-HgS), metacinnabar (β-HgS), Hg bound to organic matter ($Hg(SR)_2$), and nano-HgS were analyzed to investigate the oxidation state of Hg in the experimental samples. Methods for the synthesis of $Hg(SR)_2$ and nano-HgS have been documented previously.[14] The sample pellets and all Hg reference compounds were mounted on Kapton tape, and their Hg L_3-edge XANES spectra were obtained at the 1W1B EXAFS station of the Beijing Synchrotron Radiation Facility (BSRF) with 2.5 GeV electron energy, 250 mA electron current, and energy resolution ($\Delta E/E$) of $1-3 \times 10^{-4}$. The details for collection of spectra are described in the SI (section S2).

Sulfur K-Edge XANES Spectroscopy. Sulfur reference compounds, including elemental S (S_0), calcium sulfate dihydrate ($CaSO_4 \cdot 2H_2O$), sodium dodecyl sulfate ($NaC_{12}H_{25}SO_4$), sodium thiosulfate ($Na_2S_2O_3$), Phenyl sulfoxide ($C_{12}H_{10}S$), L-cystine ($C_6H_{12}N_2O_4S$), and L-methionine ($C_5H_{11}NO_2S$), were analyzed using medium X-ray beamline 4B7A at the BSRF. The details for collection of spectra are described in the SI (section S2).

Transmission Electron Microscopy Coupled with Energy Dispersive X-ray (TEM-EDX) Spectroscopy. Soil powders from the control and 3% NAC treatment were dispersed with 50% ethanol, mounted in a carbon-covered copper grid, and analyzed using an analytical transmission electron microscope (Tecnai G2 F20 S-TWIN TMP, FEI Co., America) operated at 200 kV. Identification of soil minerals, and NAC particles in the soil microaggregates was made with the assistance of energy dispersive X-ray (EDX) spectroscopy and selected area electron diffraction.

Data Quality Control and Assurance. Quality control for the Hg concentration in soil and plant biomass was monitored using certified soil and plant reference materials (GBW 070009 (soil) and GBW10020 (plant)) obtained from the Institute of Geophysical and Geochemical Exploration, China. Mercury recovery ranged from 90% to 102% for the plant and 92% to 106% for the soil. The analysis of plant and soil replicates showed that the relative percentage difference between replicates was <8% and <10%, respectively. Quality control for pore water samples was achieved by analyzing blanks, and samples spiked with Hg(II) standards (ICP-MS Standard, 10 mg L^{-1} Hg in nitric acid).

All data were plotted using *Origin* 15.0 software (Origin Lab Co., U.S.A.). Statistical analyses were performed using SPSS 22.0 (SPSS Inc., U.S.A.). Analysis of variance (ANOVA), and the least significant difference (LSD) tests were used to compare the treatment means at a significance level of 5% ($P < 0.05$, indicated by different lower-case characters in the figures). Partition coefficients (K_d, L kg^{-1}) were calculated as the ratio of THg concentration in soil (mg kg^{-1}) to that in pore water (mg L^{-1})[31] (eq 1).

$$K_d = \text{soil THg (mg kg}^{-1}\text{)/pore water THg (mg L}^{-1}\text{)} \times 10^{-6} \quad (1)$$

Plant Hg concentration was calculated by the summarization of Hg concentrations of root, stalk, and leaf. Bioaccumulation factor (BAF) is defined as the ratio of plant Hg concentration (mg kg^{-1}) to soil total Hg concentration (mg kg^{-1}).[32]

RESULTS AND DISCUSSION

Effect of NAC on Plant Biomass. Addition of 3% NAC significantly increased the dry weight and length of both the stem and leaf of rice plants compared to the control (Figures 1 and S3). However, NAC did not cause a significant change to the root dry weight or root volume of rice plants, relative to the control (Figures 1 and S3). These observations suggest that the addition of NAC at a dose of 3% has a beneficial effect on plant growth. Increased above-ground biomass yield of rice plants after treatment with NAC may indicate that the NAC can act as a fertilizer synergist, reducing nutrient losses, improving nutrient availability, and stimulating plant growth, as has been shown in previous studies.[17,33]

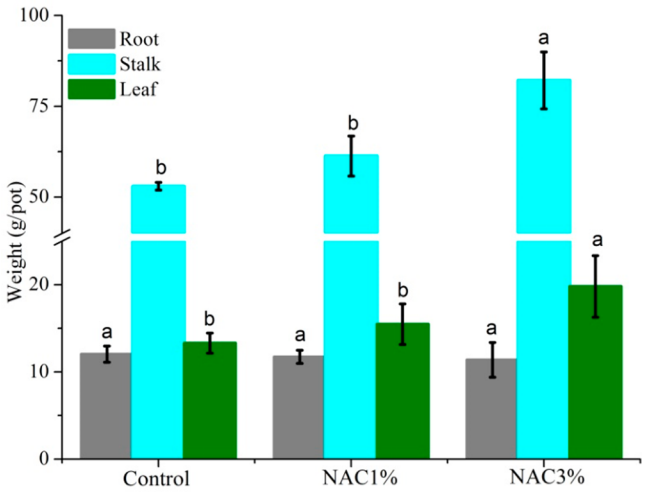

Figure 1. Dry weight of root, stalk, and leaf; differences at $P < 0.05$ tested by least significant difference in one-way analysis of variance in each biomass parameter between control and nanoactivated carbon (NAC) treatments are indicated by different small-case letters on each bar. Error bars denote standard deviation from means of three replicates (1SD).

Effect of NAC on DOC, Sulfate, Oxidation−Reduction Potential, and pH in the Pore Water. Figure 2-A shows the concentration of DOC in the pore water for all treatments throughout the rice growing season. The pore water DOC concentration in the control soil ranged from 9.3 to 49 mg L^{-1}; however, this was reduced by 9−70% and 8−86% following addition of 1% and 3% NAC, respectively with a function of the treatment rate of NAC (Figure 2-A). Adsorption of DOC by NAC might be responsible for the reduced DOC concentration in the pore water.[34] The reduction decreased after day 80, and we hypothesize this was a function of saturation of the DOC adsorption sites on NAC surface.

https://dx.doi.org/10.1021/acs.est.9b05685
Environ. Sci. Technol. 2020, 54, 2698−2706

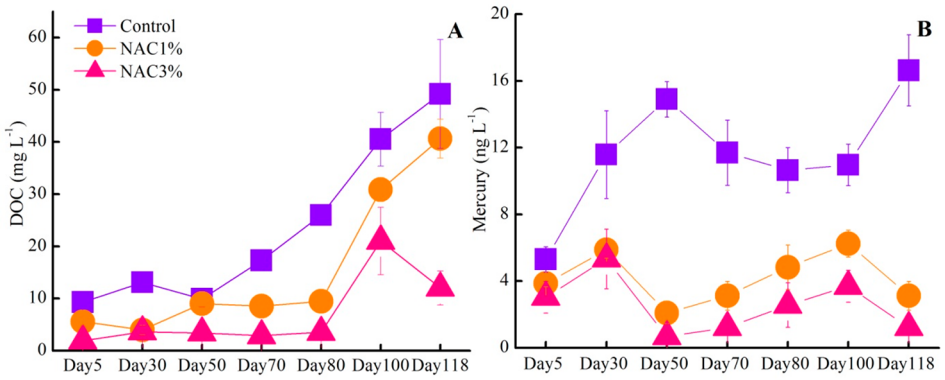

Figure 2. Concentration of dissolved organic carbon (DOC) (A) and dissolved total Hg (THg) (B) in the pore water in control and nanoactivated carbon (NAC) treatments throughout the rice growing season. Error Bars denote standard deviation from means of three replicates (1SD).

The concentration of sulfate in the pore water was significantly reduced in all the soils with time (Figure S4). This decrease for the three treatments could be a function of the microbially mediated sulfate reduction, particularly under low oxidation reduction potential (ORP) values (−389 mV to −122 mV) after 70 days (Figure S5).[35] Thus, the sulfate concentration correlated positively with ORP (Figure S6). The pH of soil pore water in the three treatments ranged from 7.4 to 8.1, and showed a gradual decrease throughout the rice growing season (Figure S7).

Effect of NAC on Hg Concentrations in the Soil and Pore Water, and on Hg Partitioning and Bioaccumulation. A minor decrease of total Hg concentration in the NAC-amended soil may be explained through dilution of the Hg concentration by NAC (Figure S8-A). Also, the volatilization of Hg through inducing Hg(II) reduction might contribute to this reduction.[20,36] Addition of NAC to soil led to a clear decrease in the Hg concentration in the pore water for both the 1% and 3% treatments relative to the control, throughout the rice growing season (Figures 2-B and S8-B). A positive correlation between Hg and DOC in the pore water demonstrates a closely biogeochemical association of these parameters[37,38] (Figure S9). Most Hg is likely bound to DOC in the pore water; the decreased DOC concentration by NAC amendment might also lead to a reduction of Hg concentration (Figure 2-A), as the removal of DOC by NAC would also remove the associated Hg complexes. Both 1% and 3% NAC addition increased Hg partitioning to bulk soils (K_d) relative to the control. The K_d value for the control soil was 11×10^3 L kg^{-1} and this increased to 22×10^3 L $kg^{-1}$for the 1% treatment, and 36×10^3 L kg^{-1} for the 3% treatment indicating that NAC promoted retention of Hg on soil solid phase constituents (Figure S8-C).

The Hg concentration in the root, stalk, leaf, bran, hull, and polished rice of rice plants growing in soil amended with NAC decreased significantly by 48−56%, 17−39%, 39−52%, 47−55%, 15−39%, and 47−63%, respectively, relative to the corresponding controls (Figures 3 and S8-D). Soil amendment with NAC significantly decreased the BAF of Hg by rice tissues compared to the control (Figure S8-E). The Hg concentration both in rice tissues and pore water showed the greatest reduction as a function of NAC, and this was more pronounced for 3% NAC treatment (Figures 2 and 3). The Hg concentration in rice tissues was correlated positively with the Hg concentration in the pore water (Figure S10-A), and thus the reduced Hg concentration in rice tissues can be

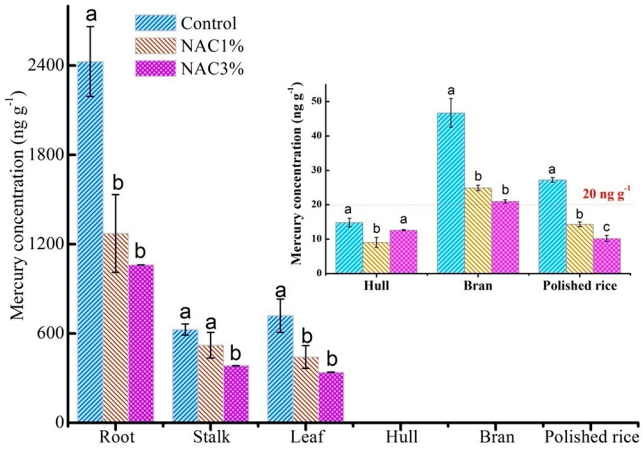

Figure 3. Mercury concentrations in the root, stalk, leaf, hull, bran, and polished rice. Significant differences tested by least significant difference in one-way analysis of variance between different rice tissues at $P < 0.05$ among control and nanoactivated carbon (NAC) treatments are indicated by different lower case letters. The red dashed line is the maximum allowable total Hg concentration (20 ng g^{-1}) in rice grain set by the Chinese government. Error Bars denote standard deviation from means of three replicates (1SD).

directly linked to the reduced Hg concentration in the pore water. A negative linear correlation between Ln(BAF) and Ln(K_d) suggests the partitioning of Hg into the soil solid phase inhibited Hg bioaccumulation (Figure S10-B). The potential for a dilution effect of Hg within the increased biomass promoted by NAC should also be considered. However, we estimate this effect to be minor relative to the change in soil chemistry because NAC addition decreased rice plant Hg accumulation, as shown by a significantly lower Hg mass in the treated rice plants as compared to control (Figure S8-F). Our work shows that NAC addition decreased Hg bioavailability, enhanced its partition to the solid phase, and reduced its bioaccumulation by rice plants.

Photomicrographs of Soil Particles Show NAC Amendment Affect the Soil Constituents Assemble. We observed chlorite-nanomagnetite-organic matter, chlorite-quartz-organic matter, and mica-organic matter microaggregates, within the control soil (Figure 4-A−C); Energy dispersive X-ray spectroscopy analysis showed that Hg presented in the organic matter matrix in those microaggregates, but its intensity was not high (Figure S11). Amendment of soil with NAC affected the soil constituents:

https://dx.doi.org/10.1021/acs.est.9b05685
Environ. Sci. Technol. 2020, 54, 2698−2706

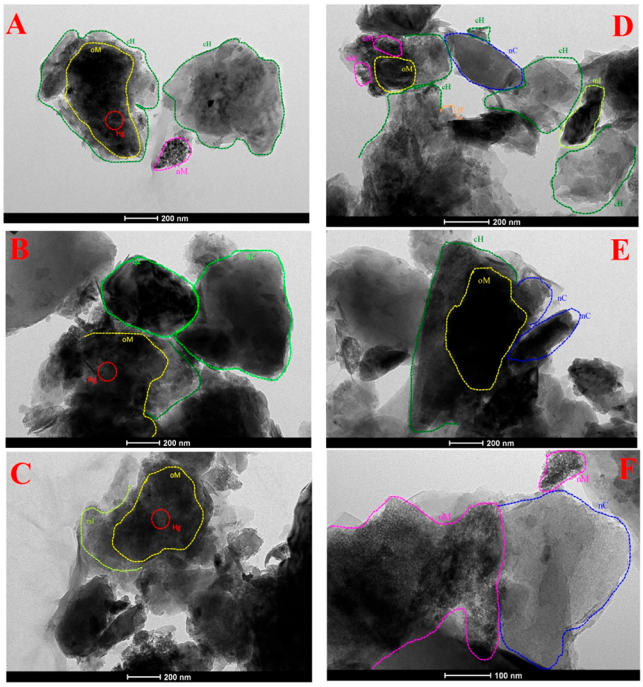

Figure 4. Transmission electron microscopy (TEM) images of microaggregates from the control (A, B, C) and soil treated with 3% nanoactivated C (D, E, F). Minerals, organic matter, and nanoactivated carbon were identified according to elemental compositions obtained by energy dispersive X-ray (TEM-EDX) spectroscopy and selected area electron diffraction. Particles circled by dashed lines with blue color are nanoactivated carbons (nC), with dark green color are chlorites (cH), with pink color are nanomagnetites (nM), with orange color are feldspars (fE), with olivedrab color are micas (mI), with yellow color are organic matter (oM), and with lime green are quartz (qZ).

NAC-chlorite-nanomagnetite, NAC-chlorite-organic matter, and NAC-nanomagnetite microaggregates were observed within the amended soil (Figures 4-D–F). Energy dispersive X-ray spectroscopy analysis showed that Hg presented in the organic matter matrix in NAC-chlorite-organic matter microaggregates as Hg–S clusters (Figure S12). Given that NAC had a close association with Hg-containing soil constituents (e.g., organic matter), Hg–S clusters presented in the NAC microaggregates, and it is likely that NAC might have facilitated immobilization of Hg by forming Hg–S clusters.

Impact of NAC on Sulfur and Mercury Speciation. The appearance of Hg–S in the microaggregates of treated soil indicated that S was likely involved in Hg speciation transformation processes. Sulfur speciation in the control and NAC treated-soil was further analyzed to understand NAC-induced changes in the speciation of sulfur in the soil. Two distinct energy edge features at 2.4762 (Figure 5-A; black arrow) and 2.4828 keV (Figure 5-A; blue arrow), were observed for spectra of the control soil, corresponding to the spectral signature of sulfoxide, and ester-sulfate sulfur.[39] A distinct energy edge feature at 2.4726 keV (Figure 5-A, red arrow) in the 3% NAC-treated soil was observed, which matches the spectral signature of elemental S.[39] However, this signature was not observed in the spectra of control soil. The linear combination fitting of the control soil showed that sulfur speciation predominately occurred as sulfoxide (92%), sulfate (1%), cystine (4%), and methionine (3%) (Figure 5-B,-D). However, in the NAC-treated soil, sulfur speciation predominately occurred as sulfoxide (74%), sulfate (5%), and elemental S (22%) (Figure 5-C,-E).

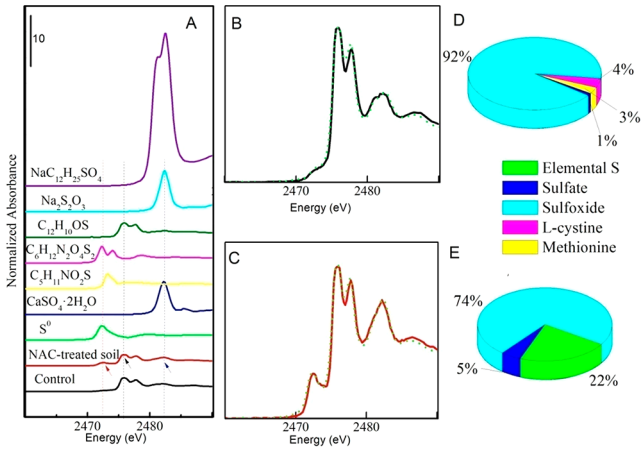

Figure 5. (A) The normalized sulfur K-edge spectra of reference compounds (elemental S (S_0), calcium sulfate dihydrate ($CaSO_4 \cdot 2H_2O$), sodium dodecyl sulfate ($NaC_{12}H_{25}SO_4$), sodium thiosulfate ($Na_2S_2O_3$), Phenyl sulfoxide ($C_{12}H_{10}S$), L-cystine ($C_6H_{12}N_2O_4S$), and L-methionine ($C_5H_{11}NO_2S$)) and two soil samples (control and nanoactivated carbon (NAC)-treated soil); (B, C) linear combination fitting results for control and treated soil, spectrum of control and the treated soil was indicated with black and orange color and the reconstructing spectrum was indicated by dash line with green color; and (D, E) pie chart shows the relative proportion of different S compounds in both control (upper apart) and the treated soil (bottom part).

Sulfur presented as sulfoxide in both the control and NAC-treated soil, which is in line with results from a previous study.[40] The elemental sulfur detected in the NAC-treated soil might have occurred as zerovalent sulfur, coexisting with polysulfides (S_n^{2-}), sulfanes (H_2S_n), hydropolysulfides (HS_n^{1-}), polythiosulfates ($S_nO_3^{2-}$), and polythionates ($S_nO_6^{2-}$)[41] present on the surface of soil minerals (e.g., ferric (hydr)oxides).[42−44] The NAC had low sulfur content, and thus the input of S^0 through NAC addition might have been small. The decrease of sulfoxide and increase of elemental S (Valence: 0) in the NAC treated soil as compared to the control may suggest the occurrence of sulfur redox reactions in the flooded paddy soil amended with NAC.[45] Sulfoxide may have accepted electrons to be reduced to S^0 in the treated soil; quinone groups of activated carbon might have acted as electron donors in this redox process.[46,47] A prerequisite for a redox reaction is a reductant and an oxidant in contact with each other. As shown in Figure 4-E, organic matter was in closely association with NAC in the soil microaggregates. It is possible that the reducing conditions (down to −389 mV) in the flooded soil of this study, and the abundance of sulfur with organic matter and minerals (e.g., chlorite and nanomagnetite), might facilitate a redox reaction between sulfur compounds and NAC. It appears that the formation of NAC-microaggregates is important for sulfur redox reaction since NAC can act as electron donors for sulfur compounds (e.g., sulfoxide).

The zerovalent sulfur (polysulfides as well) might react with Hg complexes (e.g., $Hg(SR)_n$) complex to form Hg polysulfide complexes ($Hg(S_n)SH^-$),[48,49] which can be further converted to Hg_xS_y compounds via molecular aggregation.[50] We characterized the Hg speciation in the soils by Hg L_3-edge XANES spectroscopy to verify the above hypothesis (Figure

https://dx.doi.org/10.1021/acs.est.9b05685
Environ. Sci. Technol. 2020, 54, 2698−2706

6). Mercury was predominantly present as α-HgS, nano-HgS, and $Hg(SR)_2$ both in the control and treated-soil, with

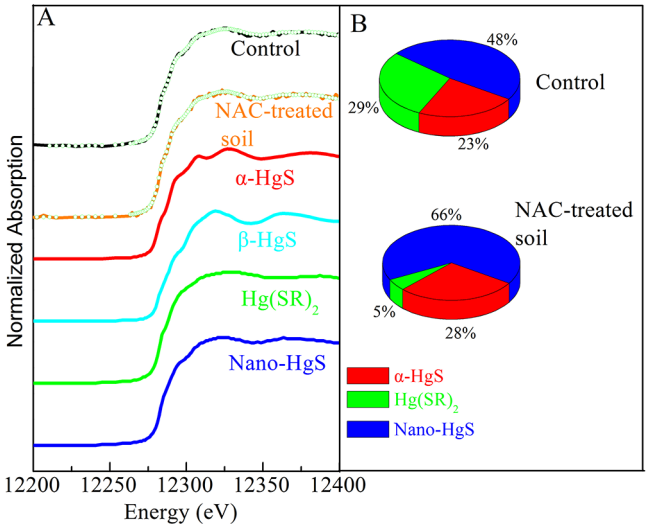

Figure 6. (A) The normalized Hg L_3-edge XANES spectra of reference compounds (α-HgS, β-HgS, $Hg(SR)_2$, and nano-HgS) and two soil samples (control and nanoactivated carbon (NAC)-treated soil); and linear combination fitting results for both control and NAC-treated soil. (B) Pie chart of the relative proportion of different Hg compounds in both control and the treated soil.

calculated proportions of 23%, 48%, 29%, and 28%, 66%, and 5%, respectively (Figure 6).

The addition of NAC changed the distribution of Hg among its chemical fractions in the soil; the proportion of nano-HgS increased by about 18%, while $Hg(SR)_2$ decreased by about 24% in the NAC-treated soil compared to the control. These findings suggest that the NAC addition induced the conversion of partial $Hg(SR)_2$ to nano-HgS supporting our hypothesis that NAC-induced sulfur speciation transformation affected Hg speciation in the soil. Nano-HgS has lower mobility and bioavailability relative to $Hg(SR)_2$ (Hg bound to soil organic matter) in the environment.[51] The immobilization of Hg to nano-HgS in the soil solid phase might have therefore reduced the Hg mobility in the pore water.

The sorption of mercuric ions by NAC through micro- and macropores is well-recognized.[36] We expect a minor role of this mechanism in our study because we assume the activated sites of NAC might be occupied by nanomagnetite and chlorite, as shown in photomicrographs (Figure 4). Furthermore, DOC was able to block activated sites of NAC,[34] as indirectly shown by the decreased DOC concentration in the pore water of the treated-soil (Figure 2-A).

Environmental Implications. Global efforts to remediate mercury have increased since the implementation of the Minamata Convention on Mercury in 2017, which aims to exclude Hg from food webs to minimize its negative effect on ecosystems. Mercury-contaminated paddy fields in many developing countries (e.g., China, Indonesia,[52] Brazil,[53] Philippines,[54] Cambodia,[55] India,[56] Thailand,[57] and Tanzania[58]) have attracted global concern because of recorded health issues in populations which consume contaminated rice grain. A key constraint on progressing mercury remediation, and mitigating exposure pathways and risk is the lack of reliable, affordable technology.[59,60] In the current work we have found for the first time that amendment of soil with nanoactivated carbon (NAC) can reduce the Hg concentration in soil pore water and its uptake by *Oryza sativa* L.

Our work shows that the Hg concentration in edible grain (polished rice) decreased to less than 20 ng g^{-1} (d.w), the safe level of Hg in foodstuffs, after soil amendment. The NAC affected the soil microaggregates, and redox reactions of sulfur and Hg compounds, and it promoted Hg immobilization under anaerobic conditions. Amendment of NAC to paddy soil could be a promising approach for reducing the risk of Hg uptake from paddy fields, and the subsequent transfer of Hg into the food chain. Rice biomass was not affected by the amendment, and there was no reduction in yield. Therefore, from an agronomic perspective, the amendment could be readily integrated with current farming systems. Soil amendment with NAC has no apparent impact to rice growth, and in this sense is preferable to conventional methods which destroy soil chemical, physical and biological properties (e.g., soil washing, stabilization/solidification, thermal desorption, and vitrification). A key advantage of the amendment is that the costs of production and use are low. A cost-effectiveness analysis of using NAC for Hg-contaminated farmlands remediation is displayed in the SI (section S3). Activated carbon is a commercially available product made from waste material, and a sufficient amount is available to treat the large scale of contaminated paddy soils. Our results support the technical feasibility of using NAC as a soil amendment for the remediation of Hg-contaminated paddy soils worldwide, especially in developing regions (e.g., Guizhou in China) where large contaminated paddy fields are under cultivation and need urgent, effective, remedial intervention. Our findings provide mechanistic insight in future research toward the use of NAC to immobilize Hg in anaerobic environments.

Further studies are necessary to upscaling of our method to field. For example, the stability of NAC-microaggregates in changing environments (e.g., redox fluctuations), the mechanisms of NAC-induced redox changes in sulfur chemistry in soils, the long-term stability of NAC immobilized Hg, determining an optimal application form and rate of NAC, and the effect of NAC on Hg^0 emission from soils.

■ ASSOCIATED CONTENT

Supporting Information

The Supporting Information is available free of charge at https://pubs.acs.org/doi/10.1021/acs.est.9b05685.

More details on soil, liquid, and solid sample analysis; discussion for cost-effectiveness analysis for nanoactivated carbon (NAC); tables for properties of the studied soil and NAC, not shown in the main text; figures showing iron speciation in the soil characterized by X-ray absorption near edge structure (XANES) spectroscopy, TEM image of NAC, the length of root and above ground tissue and the volume of root, concentrations of sulfate in the pore water throughout the rice growing season, ORP value in the pore water throughout the rice growing season, the relationship between ORP and sulfate in the pore water, the pH value in the pore water throughout the rice growing season, the relationship between dissolved Hg and dissolved organic carbon (DOC) concentration in the pore water, the relationship between Hg contents in tissues of rice plant and Hg concentration in the pore water, the relationship between K_d and BAF, EDX

https://dx.doi.org/10.1021/acs.est.9b05685
Environ. Sci. Technol. 2020, 54, 2698−2706

spectra for the soil microaggregates, identification of Hg−S clusters in 3% nanoactivated carbon treatment using transmission electron microscopy coupled with energy dispersive X-ray (TEM-EDX) spectroscopy, and results of comparison of soil total Hg content, pore water total dissolved Hg, soil/water partition coefficients (K_d), plant tissue Hg contents, BAF, plant tissues Hg mass, between control and nanoactivated carbon (NAC) treatments (PDF)

AUTHOR INFORMATION

Corresponding Authors

Jianxu Wang − *State Key Laboratory of Environmental Geochemistry, Institute of Geochemistry, Chinese Academy of Sciences, 550081 Guiyang, P. R. China; University of Wuppertal, School of Architecture and Civil Engineering, Institute of Foundation Engineering, Water- and Waste-Management, Laboratory of Soil- and Groundwater-Management, 42285 Wuppertal, Germany; CAS Center for Excellence in Quaternary Science and Global Change, Xi'an 710061, P. R. China*; Email: wangjianxu@vip.gyig.ac.cn

Xinbin Feng − *State Key Laboratory of Environmental Geochemistry, Institute of Geochemistry, Chinese Academy of Sciences, 550081 Guiyang, P. R. China; CAS Center for Excellence in Quaternary Science and Global Change, Xi'an 710061, P. R. China*; orcid.org/0000-0002-7462-8998; Email: fengxinbin@vip.skleg.cn

Authors

Sabry M. Shaheen − *University of Wuppertal, School of Architecture and Civil Engineering, Institute of Foundation Engineering, Water- and Waste-Management, Laboratory of Soil- and Groundwater-Management, 42285 Wuppertal, Germany; King Abdulaziz University, Faculty of Meteorology, Environment, and Arid Land Agriculture, Department of Arid Land Agriculture, Jeddah 21589, Kingdom of Saudi Arabia; University of Kafrelsheikh, Faculty of Agriculture, Department of Soil and Water Sciences, 33516 Kafr El-Sheikh, Egypt*

Christopher W. N. Anderson − *Environmental Sciences, School of Agriculture and Environment, Massey University, 4442 Palmerston North, New Zealand*

Ying Xing − *School of Chemistry and Materials Science, Guizhou Normal University, 550001 Guiyang, P. R. China*

Shirong Liu − *State Key Laboratory of Environmental Geochemistry, Institute of Geochemistry, Chinese Academy of Sciences, 550081 Guiyang, P. R. China*

Jicheng Xia − *State Key Laboratory of Environmental Geochemistry, Institute of Geochemistry, Chinese Academy of Sciences, 550081 Guiyang, P. R. China*

Jörg Rinklebe − *University of Wuppertal, School of Architecture and Civil Engineering, Institute of Foundation Engineering, Water- and Waste-Management, Laboratory of Soil- and Groundwater-Management, 42285 Wuppertal, Germany; University of Sejong, Department of Environment, Energy and Geoinformatics, Guangjin-Gu, Seoul 05006, Republic of Korea*; orcid.org/0000-0001-7404-1639

Complete contact information is available at: https://pubs.acs.org/10.1021/acs.est.9b05685

Notes

The authors declare no competing financial interest.

ACKNOWLEDGMENTS

This study was financed by the National Natural Science Foundation of China [grant nos. 41573082, 41703116]; Guizhou Science and Technology Project [grant no. [2017] 5726-23], and the opening Fund of the State Key Laboratory of Environmental Geochemistry [SKLEG2017907, SKLEG2017912]. W.J.X. was supported by the German Alexander von Humboldt Foundation (ref 3.5-1186537-CHN-HFST-P). Many thanks go to the 1W1B, 4B7A, and 4B7B beam stations at Beijing Synchrotron Radiation Facility for supporting Hg L_3-edge, S K-edge, and Fe L-edge XANES spectroscopy analysis [Nos. 2017-BEPC-PT-001048, 2018-BEPC-PT-001491, and 2018-BEPC-PT-001459].

REFERENCES

(1) Hsu-Kim, H.; Eckley, C. S.; Achá, D.; Feng, X.; Gilmour, C. C.; Jonsson, S.; Mitchell, C. P. J. Challenges and opportunities for managing aquatic mercury pollution in altered landscapes. *Ambio* **2018**, *47* (2), 141−169.

(2) Chen, C. Y.; Driscoll, C. T.; Evers, D. C.; Lambert, K. F.; Kamman, N. C.; Munson, R. K.; Holsen, T. M.; Han, Y.-J. Mercury Contamination in Forest and Freshwater Ecosystems in the Northeastern United States. *BioScience* **2007**, *57* (1), 17−28.

(3) Wang, J. X.; Feng, X. B.; Anderson, C. W. N.; Xing, Y.; Shang, L. H. Remediation of mercury contaminated sites - A review. *J. Hazard. Mater.* **2012**, *221*, 1−18.

(4) Beckers, F.; Rinklebe, J. Cycling of mercury in the environment: Sources, fate, and human health implications: A review. *Crit. Rev. Environ. Sci. Technol.* **2017**, *47* (9), 693−794.

(5) Wang, J.; Shaheen, S. M.; Swertz, A.-C.; Rennert, T.; Feng, X.; Rinklebe, J. Sulfur-modified organoclay promotes plant uptake and affects geochemical fractionation of mercury in a polluted floodplain soil. *J. Hazard. Mater.* **2019**, *371*, 687−693.

(6) Rothenberg, S. E.; Windham-Myers, L.; Creswell, J. E. Rice methylmercury exposure and mitigation: A comprehensive review. *Environ. Res.* **2014**, *133*, 407−423.

(7) Bandumula, N. Rice Production in Asia: Key to Global Food Security. *Proc. Natl. Acad. Sci., India, Sect. B* **2018**, *88* (4), 1323−1328.

(8) Feng, X.; Qiu, G. Mercury pollution in Guizhou, Southwestern China — An overview. *Sci. Total Environ.* **2008**, *400* (1), 227−237.

(9) Payne, R. B.; Ghosh, U.; May, H. D.; Marshall, C. W.; Sowers, K. R. A Pilot-Scale Field Study: In Situ Treatment of PCB-Impacted Sediments with Bioamended Activated Carbon. *Environ. Sci. Technol.* **2019**, *53* (5), 2626−2634.

(10) O'Connor, D.; Hou, D.; Ok, Y. S.; Mulder, J.; Duan, L.; Wu, Q.; Wang, S.; Tack, F. M. G.; Rinklebe, J. Mercury speciation, transformation, and transportation in soils, atmospheric flux, and implications for risk management: A critical review. *Environ. Int.* **2019**, *126*, 747−761.

(11) Merly, C.; Hube, D. Remediation of Mercury-Contaminated Sites. In Project No. SN-03/08. Available at https://docplayer.net/18898131-Remediation-of-mercury-contaminated-sites.html 2014.

(12) Wang, Y.; Wei, Z.; Zeng, Q.; Zhong, H. Amendment of sulfate with Se into soils further reduces methylmercury accumulation in rice. *J. Soils Sediments* **2016**, *16* (12), 2720−2727.

(13) Wang, J.; Xing, Y.; Xie, Y.; Meng, Y.; Xia, J.; Feng, X. The use of calcium carbonate-enriched clay minerals and diammonium phosphate as novel immobilization agents for mercury remediation: Spectral investigations and field applications. *Sci. Total Environ.* **2019**, *646*, 1615−1623.

(14) Liu, T.; Wang, J.; Feng, X.; Zhang, H.; Zhu, Z.; Cheng, S. Spectral insight into thiosulfate-induced mercury speciation transformation in a historically polluted soil. *Sci. Total Environ.* **2019**, *657*, 938−944.

(15) Li, Y. F.; Zhao, J. T.; Li, Y. Y.; Li, H. J.; Zhang, J. F.; Li, B.; Gao, Y. X.; Chen, C. Y.; Luo, M. Y.; Huang, R.; Li, J. The concentration of selenium matters: a field study on mercury accumulation in rice by

selenite treatment in qingzhen, Guizhou, China. *Plant Soil* **2015**, *391* (1−2), 195−205.
(16) Wang, J. X.; Xia, J. C.; Feng, X. B. Screening of chelating ligands to enhance mercury accumulation from historically mercury-contaminated soils for phytoextraction. *J. Environ. Manage.* **2017**, *186*, 233−239.
(17) Zaytseva, O.; Neumann, G. Carbon nanomaterials: production, impact on plant development, agricultural and environmental applications. *Chem. Biol. Technol.* **2016**, *3* (1), 17.
(18) Shaheen, S. M.; Rinklebe, J. Impact of emerging and low cost alternative amendments on the (im)mobilization and phytoavailability of Cd and Pb in a contaminated floodplain soil. *Eco Eng.* **2015**, *74*, 319−326.
(19) Abel, S.; Akkanen, J. A Combined Field and Laboratory Study on Activated Carbon-Based Thin Layer Capping in a PCB-Contaminated Boreal Lake. *Environ. Sci. Technol.* **2018**, *52* (8), 4702−4710.
(20) Gilmour, C. C.; Riedel, G. S.; Riedel, G.; Kwon, S.; Landis, R.; Brown, S. S.; Menzie, C. A.; Ghosh, U. Activated Carbon Mitigates Mercury and Methylmercury Bioavailability in Contaminated Sediments. *Environ. Sci. Technol.* **2013**, *47* (22), 13001−13010.
(21) Zhu, J.; Deng, B.; Yang, J.; Gang, D. Modifying activated carbon with hybrid ligands for enhancing aqueous mercury removal. *Carbon* **2009**, *47* (8), 2014−2025.
(22) Bessinger, B. A.; Marks, C. D. Treatment of mercury-contaminated soils with activated carbon: A laboratory, field, and modeling study. *Remed J.* **2010**, *21* (1), 115−135.
(23) Lloyd-Jones, P. J.; Rangel-Mendez, J. R.; Streat, M. Mercury Sorption from Aqueous Solution by Chelating Ion Exchange Resins, Activated Carbon and a Biosorbent. *Process Saf. Environ. Prot.* **2004**, *82* (4), 301−311.
(24) Ding, D.; Zhao, Y.; Fang, Y.; Feng, H. Effect of addition of activated carbon on soil pore structure. *Agr Res. Arid Areas* **2018**, *36* (1), 36−42. (in Chinese)
(25) Liang, B.; Lehmann, J.; Sohi, S. P.; Thies, J. E.; O'Neill, B.; Trujillo, L.; Gaunt, J.; Solomon, D.; Grossman, J.; Neves, E. G.; Luizão, F. J. Black carbon affects the cycling of non-black carbon in soil. *Org. Geochem.* **2010**, *41* (2), 206−213.
(26) Chinese National Environment Protect Agency. Environmental quality standard for soils (in Chinese); GB15618−1995, 1−6. 1995.
(27) Kabata-Pendias, A. *Trace Elements in Soils and Plants*, 4th ed., CRC Press: Boca Raton, FL, 2011.
(28) Lu, R. *Chemical Analysis Method of Agricultural Soil*; China Agricultural Science Press: Beijing, 2000 (in Chinese).
(29) Wang, J. X.; Feng, X. B.; Anderson, C. W. N.; Wang, H.; Zheng, L. R.; Hu, T. D. Implications of Mercury Speciation in Thiosulfate Treated Plants. *Environ. Sci. Technol.* **2012**, *46* (10), 5361−5368.
(30) Sholupov, S.; Pogarev, S.; Ryzhov, V.; Mashyanov, N.; Stroganov, A. Zeeman atomic absorption spectrometer RA-915+for direct determination of mercury in air and complex matrix samples. *Fuel Process. Technol.* **2004**, *85* (6−7), 473−485.
(31) Lyon, B. F.; Ambrose, R.; Rice, G.; Maxwell, C. J. Calculation of soil-water and benthic sediment partition coefficients for mercury. *Chemosphere* **1997**, *35* (4), 791−808.
(32) Wang, J. X.; Feng, X. B.; Anderson, C. W. N.; Qiu, G. L.; Ping, L.; Bao, Z. D. Ammonium thiosulphate enhanced phytoextraction from mercury contaminated soil - Results from a greenhouse study. *J. Hazard. Mater.* **2011**, *186* (1), 119−127.
(33) Bhati, A.; Gunture; Tripathi, K. M.; Singh, A.; Sarkar, S.; Sonkar, S. K. Exploration of nano carbons in relevance to plant systems. *New J. Chem.* **2018**, *42* (20), 16411−16427.
(34) Shimabuku, K. K.; Kennedy, A. M.; Mulhern, R. E.; Summers, R. S. Evaluating Activated Carbon Adsorption of Dissolved Organic Matter and Micropollutants Using Fluorescence Spectroscopy. *Environ. Sci. Technol.* **2017**, *51* (5), 2676−2684.
(35) Wind, T.; Stubner, S.; Conrad, R. Sulfate-reducing Bacteria in Rice Field Soil and on Rice Roots. *Syst. Appl. Microbiol.* **1999**, *22* (2), 269−279.
(36) Huang, C. P.; Blankenship, D. W. The removal of mercury(II) from dilute aqueous solution by activated carbon. *Water Res.* **1984**, *18* (1), 37−46.
(37) Ravichandran, M. Interactions between mercury and dissolved organic matter - a review. *Chemosphere* **2004**, *55* (3), 319−331.
(38) Frohne, T.; Rinklebe, J.; Langer, U.; Du Laing, G.; Mothes, S.; Wennrich, R. Biogeochemical factors affecting mercury methylation rate in two contaminated floodplain soils. *Biogeosciences* **2012**, *9* (1), 493−507.
(39) Prietzel, J.; Botzaki, A.; Tyufekchieva, N.; Brettholle, M.; Thieme, J.; Klysubun, W. Sulfur Speciation in Soil by S K-Edge XANES Spectroscopy: Comparison of Spectral Deconvolution and Linear Combination Fitting. *Environ. Sci. Technol.* **2011**, *45* (7), 2878−2886.
(40) Zhao, F. J.; Lehmann, J.; Solomon, D.; Fox, M. A.; McGrath, S. P. Sulphur speciation and turnover in soils: evidence from sulphur K-edge XANES spectroscopy and isotope dilution studies. *Soil Biol. Biochem.* **2006**, *38* (5), 1000−1007.
(41) Fabbri, D.; Locatelli, C.; Snape, C. E.; Tarabusi, S. Sulfur speciation in mercury-contaminated sediments of a coastal lagoon: the role of elemental sulfur. *J. Environ. Monit.* **2001**, *3* (5), 483−486.
(42) Helz, G. R. Activity of zero-valent sulfur in sulfidic natural waters. *Geochem. Trans.* **2014**, *15* (1), 13−13.
(43) Wan, M.; Shchukarev, A.; Lohmayer, R.; Planer-Friedrich, B.; Peiffer, S. Occurrence of surface polysulfides during the interaction between ferric (hydr) oxides and aqueous sulfide. *Environ. Sci. Technol.* **2014**, *48* (9), 5076−5084.
(44) Kamyshny, A.; Zilberbrand, M.; Ekeltchik, I.; Voitsekovski, T.; Gun, J.; Lev, O. Speciation of Polysulfides and Zerovalent Sulfur in Sulfide-rich Water Wells in Southern and Central Israel. *Aquat. Geochem.* **2008**, *14* (2), 171−192.
(45) Zhao, F.; Rahunen, N.; Varcoe, J. R.; Chandra, A.; Avignone-Rossa, C.; Thumser, A. E.; Slade, R. C. T. Activated Carbon Cloth as Anode for Sulfate Removal in a Microbial Fuel Cell. *Environ. Sci. Technol.* **2008**, *42* (13), 4971−4976.
(46) Saquing, J. M.; Yu, Y.-H.; Chiu, P. C. Wood-Derived Black Carbon (Biochar) as a Microbial Electron Donor and Acceptor. *Environ. Sci. Technol. Lett.* **2016**, *3* (2), 62−66.
(47) Garten, V.; Weiss, D. The quinone-hydroquinone character of activated carbon and carbon black. *Aust. J. Chem.* **1955**, *8* (1), 68−95.
(48) Paquette, K. E.; Helz, G. R. Inorganic Speciation of Mercury in Sulfidic Waters: The Importance of Zero-Valent Sulfur. *Environ. Sci. Technol.* **1997**, *31* (7), 2148−2153.
(49) Kampalath, R. A.; Lin, C.-C.; Jay, J. A. Influences of Zero-Valent Sulfur on Mercury Methylation in Bacterial Cocultures. *Water, Air, Soil Pollut.* **2013**, *224* (2), 1399−1413.
(50) Manceau, A.; Wang, J.; Rovezzi, M.; Glatzel, P.; Feng, X. Biogenesis of Mercury−Sulfur Nanoparticles in Plant Leaves from Atmospheric Gaseous Mercury. *Environ. Sci. Technol.* **2018**, *52* (7), 3935−3948.
(51) Gai, K.; Hoelen, T. P.; Hsu-Kim, H.; Lowry, G. V. Mobility of Four Common Mercury Species in Model and Natural Unsaturated Soils. *Environ. Sci. Technol.* **2016**, *50* (7), 3342−3351.
(52) Krisnayanti, B. D.; Anderson, C. W. N.; Utomo, W. H.; Feng, X.; Handayanto, E.; Mudarisna, N.; Ikram, H. Assessment of environmental mercury discharge at a four-year-old artisanal gold mining area on Lombok Island, Indonesia. *J. Environ. Monit.* **2012**, *14* (10), 2598−2607.
(53) Kütter, V. T.; Kütter, M. T.; Silva-Filho, E. V.; Marques, E. D.; Gomes, O. V. d. O.; Mirlean, N. Mercury bioaccumulation in fishes of a paddy field in Southern of Brazil. *Acta Limnol. Bras.* **2015**, *27*, 191−201.
(54) Appleton, J. D.; Weeks, J. M.; Calvez, J. P. S.; Beinhoff, C. Impacts of mercury contaminated mining waste on soil quality, crops, bivalves, and fish in the Naboc River area, Mindanao, Philippines. *Sci. Total Environ.* **2006**, *354* (2), 198−211.
(55) Cheng, Z.; Wang, H.-S.; Du, J.; Sthiannopkao, S.; Xing, G.-H.; Kim, K.-W.; Yasin, M. S. M.; Hashim, J. H.; Wong, M.-H. Dietary

https://dx.doi.org/10.1021/acs.est.9b05685
Environ. Sci. Technol. 2020, 54, 2698−2706

exposure and risk assessment of mercury via total diet study in Cambodia. *Chemosphere* **2013**, *92* (1), 143−149.
(56) Lenka, M.; Panda, K. K.; Panda, B. B. Monitoring and assessment of mercury pollution in the vicinity of a chloralkali plant. IV. Bioconcentration of mercury in in situ aquatic and terrestrial plants at Ganjam, India. *Arch. Environ. Contam. Toxicol.* **1992**, *22* (2), 195−202.
(57) Pataranawat, P.; Parkpian, P.; Polprasert, C.; Delaune, R.; Jugsujinda, A. Mercury emission and distribution: Potential environmental risks at a small-scale gold mining operation, Phichit Province, Thailand. *J. Environ. Sci. Health, Part A: Toxic/Hazard. Subst. Environ. Eng.* **2007**, *42* (8), 1081−1093.
(58) Taylor, H.; Appleton, J.; Lister, R.; Smith, B.; Chitamweba, D.; Mkumbo, O.; Machiwa, J.; Tesha, A.; Beinhoff, C. Environmental assessment of mercury contamination from the Rwamagasa artisanal gold mining centre, Geita District, Tanzania. *Sci. Total Environ.* **2005**, *343* (1−3), 111−133.
(59) Xing, Y.; Wang, J.; Shaheen, S. M.; Feng, X.; Chen, Z.; Zhang, H.; Rinklebe, J. Mitigation of mercury accumulation in rice using rice hull-derived biochar as soil amendment: A field investigation. *J. Hazard. Mater.* **2019**, 121747.
(60) Wang, J.; Sun, X.; Xing, Y.; Xia, J.; Feng, X. Immobilization of mercury and arsenic in a mine tailing from a typical Carlin-type gold mining site in southwestern part of China. *J. Cleaner Prod.* **2019**, *240*, 118171.

https://dx.doi.org/10.1021/acs.est.9b05685
Environ. Sci. Technol. 2020, 54, 2698−2706